Characterization of the Nuclear Deformation Caused by Changes in Endothelial Cell Shape

Ronald P. Jean
Darren S. Gray
Alexander A. Spector
Christopher S. Chen
e-mail: aspector@bme.jhu.edu

Department of Biomedical Engineering,
The Johns Hopkins University,
Baltimore, MD 21205

We investigated the mechanotransduction pathway in endothelial cells between their nucleus and adhesions to the extracellular matrix. First, we measured nuclear deformations in response to alterations of cell shape as cells detach from a flat surface. We found that the nuclear deformation appeared to be in direct and immediate response to alterations of the cell adhesion area. The nucleus was then treated as a neo-Hookean compressible material, and we estimated the stress associated with the cytoskeleton and acting on the nucleus during cell rounding. With the obtained stress field, we estimated the magnitude of the forces deforming the nucleus. Considering the initial and final components of this adhesion-cytoskeleton-nucleus force transmission pathway, we found our estimate for the internal forces acting on the nucleus to be on the same order of magnitude as previously measured traction forces, suggesting a direct mechanical link between adhesions and the nucleus. [DOI: 10.1115/1.1800559]

Keywords: Cell Mechanics, Mechanics of the Nucleus, Cytoskeletal Forces, Endothelial Cells

1 Introduction

Cells of all types are constantly being exposed to external forces within their physiological environment [1–3]. While these external loads have been shown to regulate normal cell function, the mechanism by which these external forces elicit a cellular response (*mechanotransduction*) is still not fully understood. There are a number of possible locations where mechanotransduction might occur within an endothelial cell. Shear stress on the apical surface has been shown to activate G-proteins, thereby leading to the activation of various messenger molecules downstream of this pathway [4], and such stress also affects basal adhesions [5,6]. At the adhesion surface, forces are transmitted through integrin transmembranous receptors, resulting in the activation of various messenger molecules that participate in different signaling pathways [7]. Mechanotransduction may also occur within or near the nucleus [8]. The observation that endothelial cells possess direct mechanical connections between integrins, the cytoskeleton, and the nucleus [9] suggests a possible direct line of force transfer between the surface of the cell and the nucleus. Moreover, modulation of nuclear shape has been suggested to affect both protein synthesis and gene expression [10].

There has been much investigation into the mechanics of the elements within this pathway between integrins and the nucleus, particularly cell adhesions and the cytoskeleton. When a cell adheres to a surface, it exerts traction forces to balance its internal forces generated by contraction of the cytoskeleton [11]. The protein family of integrins is responsible for connecting the cell to the extracellular environment. The traction force of various cell types have been measured, and most cells appear to generate traction forces in the range of tens to hundreds of nanoNewtons [12–16]. In response to externally applied forces, the cytoskeleton of cells is believed to serve as a network of force transfer within the fluid-like cytoplasm [8,17,18]. The mechanical properties of actin (micro) filaments and intermediate filaments (IF's) have been investigated at both the cellular and molecular levels. The estimated magnitude of force during actin-myosin contraction is a few piconewtons [19]. In response to shear stress, intermediate filaments have been observed to experience significant displacements [20]. Computational studies have begun to show detailed three-dimensional strains of the intermediate filament network [21]. There have been a number of important studies of the passive and active properties of the cytoskeleton and/or cytoplasm in a number of cells [22–29]. Nevertheless, the mechanism of force generation by the cytoskeletal network has not been fully understood.

Recently, measurements of the mechanical properties of the cell nucleus have become available. Chondrocyte nuclei have been measured to be 3–4 times stiffer than cytoplasm [30]. Deformations of endothelial cell cytoplasm and nucleus during micropipette manipulation also suggest nuclear material is stiffer than cytoplasm [9]. Lastly, using a microplate compression technique to obtain more quantitative estimates for the stiffness of endothelial cell nuclei, another study found the stiffness of these nuclei to be about 5000 Pa—nearly 10 times as stiff as the corresponding cytoplasm [31]. The Young's modulus for the cytoplasm (500 Pa) in [31] is consistent with the effective Young's modulus for the endothelial cell [32].

Studies of the mechanical properties of the nucleus, as well as computational and theoretical analyses have been performed to investigate the effect of external forces on the cell nucleus. Recently, a computational model was developed to test the transmission of external force to the nucleus via cytoskeletal fibers [33]. The magnitude and frequency of external forces were varied in a model consisting of a cell surface, a randomly-generated fiber mesh, and internal nucleus. The findings of the simulation went beyond establishing the idea of direct cytoskeletal connections between the nucleus and the surface: it was demonstrated that these cytoskeletal fibers could also reliably transmit force to the nucleus on the order of seconds [33]. Additionally, a theoretical analysis of endothelial cells exposed to fluid flow has suggested that the cells adapt by minimizing the magnitude of force acting on the nucleus [34].

One approach used to study the response of the nucleus to external cellular forces is by partially detaching cells from their substrate to cause cell rounding. Early studies on nuclear deformations measured projected nuclear area and cell adhesion area in response to trypsin [35] and addition of ATP [36] to increase contractility of the cell. Both experiments showed a decrease in projected nuclear area in response to cell rounding. Unfortunately, the

Contributed by the Bioengineering Division for publication in the JOURNAL OF BIOMECHANICAL ENGINEERING. Manuscript received by the Bioengineering Division May 26, 2004; revision received June 1, 2004. Associate Editor: C. Dong.

 Copyright © 2004 by ASME

nuclear displacements or stretches, which must be known for a mechanical analysis were not measured in these studies and could not be extracted from the reported results.

Here, we investigate deformations of the nucleus resulting from cell rounding, and estimate the mechanical forces acting on the nucleus. Adhesion area was altered by disruption of integrin binding. Then, we measure changes in the projected cell area (apparent adhesion area) as cells round up, and calculate the corresponding stretches of the nucleus. We found that stretches of the major and minor axes of the projected nuclear area had the same mean value (0.69). Additionally, the projected nuclear area and cell area both decrease at a similar rate, suggesting that the nucleus deforms directly (and without delay) in response to changes in adhesion area. We extend our experimental findings with a theoretical consideration of the nucleus: we derive the stresses responsible for the nuclear deformation and convert them into ''equivalent'' forces. In our analysis of cell rounding, we consider the spread and round states of the nucleus as the reference and final states, respectively. On that basis, we interpret the forces deforming the nucleus as opposite to those that are produced by the cytoskeleton during cell spreading. Thus, we can compare our estimates with traction forces at adhesion sites, and we found them to be on the same order of magnitude. Our analysis of the deformation of the nucleus and the surrounding components of the cell is an important component for future considerations of mechanotransduction. Understanding the forces present within and on the adhesion surface of endothelial cells has direct significance to wound healing, angiogenesis, and endothelial barrier dysfunction.

2 Materials and Methods

2.1 Cell Culture. Bovine pulmonary artery endothelial cells (BPAECs, VEC Technologies) were cultured in low glucose DMEM (Gibco) with 10% calf serum, 100 units/mL penicillin, 100 μg/mL streptomycin, and 2 mM glutamine (Gibco) under standard tissue culture conditions. In preparation for experiments, cells between passages 12 and 14 were seeded at a density of $\sim$170 cells/mm^2 into 35 mm glass bottom microwell dishes (MatTek Corp.).

In order to image the nuclear area, cells were allowed to spread for 10 h, and stained for 2 h with 1 μg/ml Hoescht 33258 nucleic acid stain (Molecular Probes) in PBS, and rinsed with PBS. We induced cell rounding with 0.006% and 0.017% trypsin (Gibco) in PBS.

2.2 Microscopy and Image Analysis. A Nikon TE-200 microscope was used to acquire phase-contrast images of cells and fluorescence images of their nuclei using a 40$\times$ objective with an exposure time of 200 milliseconds. Cells were imaged every 15–30 s until they rounded up, becoming spherical in shape. To obtain quantitative information about the cell area, cells were manually outlined using Adobe Photoshop 5.0. The outlined and filled cell areas were then thresholded to create a binary (black-and-white) image, with black regions representing background, and white regions representing cell adhesion area. To obtain nuclear stretches, images of cell nuclei were processed using a despeckle filter to remove background noise and then thresholded. Cell and nuclear areas were obtained by automatic counting of pixels in the binary images by MatLab. Cells and nuclei were characterized as being in the rounded state when there was less than 4% relative nuclear area change between image frames of 3 consecutive images, and the middle image of the 3 was defined as the round state.

3 Measurements and Experimental Results

We were interested in measuring nuclear stretches during cell rounding. Observing that rotations of the nucleus during cell rounding are small, the major (direction 1) and minor (direction 2) axes can be considered the principal axes (Fig. 1). We define the principal stretch as

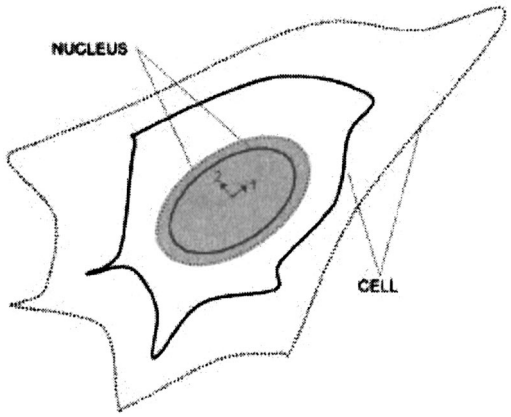

Fig. 1 Sketch of the projected nuclear and cell areas in the spread (dashed line) and round (solid line) states. Principal directions 1 and 2 correspond to the major and minor axes of the nucleus.

$$\lambda_i = \frac{d_i}{d_i^o} \tag{1}$$

where λ_i is the stretch, d_i is the current diameter in direction i, and d_i^o is the initial diameter in direction i, for $i=1, 2$. The product of stretches 1 and 2 equals the relative change in projected area of the nucleus (A_n), given by

$$\lambda_1 \lambda_2 = A_n \tag{2}$$

To cause a decrease in the cell adhesion area, we used trypsin, an enzyme that releases cell adhesions. We measured the projected area of the cell, and assuming a homogenous distribution of focal contacts across the basal surface of the cell, this can be interpreted as the apparent cell adhesion area. Two concentrations of trypsin (0.006% and 0.017%) were used in our experiments to determine if the nuclear stretches were trypsin concentration-dependent. Representative pictures of the acquired images from the cell rounding experiments are shown in Figs. 2 and 3. In Fig. 2, a representative phase-contrast image of endothelial cells is shown for 2 states during the cell rounding, as well as the same figures after image processing as described in the Methods. Figure 3 depicts the corresponding fluorescence subfield of nuclei for the same two states during cell rounding, along with the images after processing.

Endothelial cell rounding is stochastic, so that some cells round up faster than others. Hence, some of the image fields contain cells that are rounded and cells that are still somewhat spread. To see if there was any rate-dependence to the nuclear deformations, we compared all of our data with a normalized time parameter, so that the time of each cell rounding event was mapped to a relative time of 0–1.

Figure 4 shows the nuclear stretch as a function of relative time for the two concentrations of trypsin. Only one stretch is shown because we found that the mean value of the stretch in direction 1 and 2 was the same for full rounding (0.69). In Fig. 5, we plot the relative change in projected nuclear area as a function of the relative time parameter for the two concentrations of trypsin. Figure 6 shows the adhesion area ratio as a function of the relative time parameter. We compared the nuclear response (Figs. 4 and 5) to the cell adhesion change (Fig. 6) by introducing a transfer ratio, which we defined as the ratio of the nuclear area ratio to the adhesion area ratio for an individual cell. This parameter provides a means to compare the relative timecourses of the cellular and nuclear deformations. The transfer ratio as a function of relative time is provided in Fig. 7.

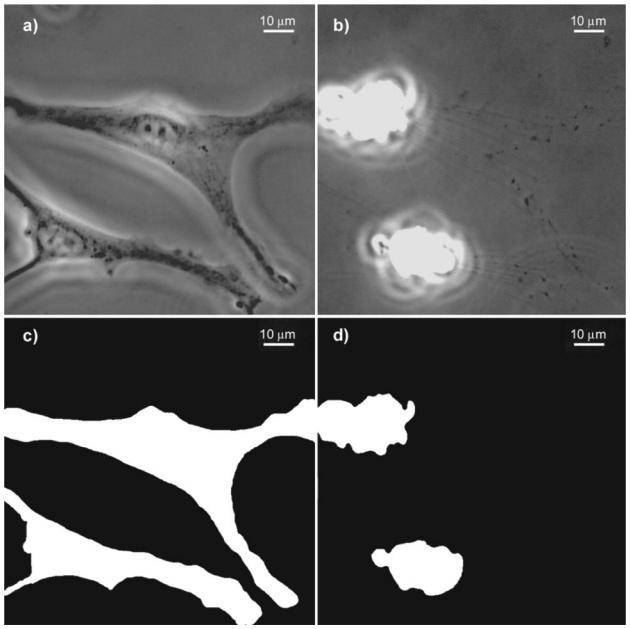

Fig. 2 Representative phase-contrast images of the endothelial cell at time (*a*) $t=0$ s, and (*b*) $t=180$ s; and the corresponding processed images for (*c*) $t=0$ s, and (*d*) $t=180$ s. Adhesions were disrupted using a chemical treatment (trypsin).

These data were divided up into 5 bins based upon the value of the relative time parameter, representing different states of the cell in the nuclear deformation path. The means and standard deviations of the nuclear area ratio for these different states were calculated for the two experiments with different trypsin concentrations. The combined data was also considered. These statistics are provided in Table 1. We also calculated the means and standard deviations for the different states during cell rounding of the cell adhesion area, presented in Table 2.

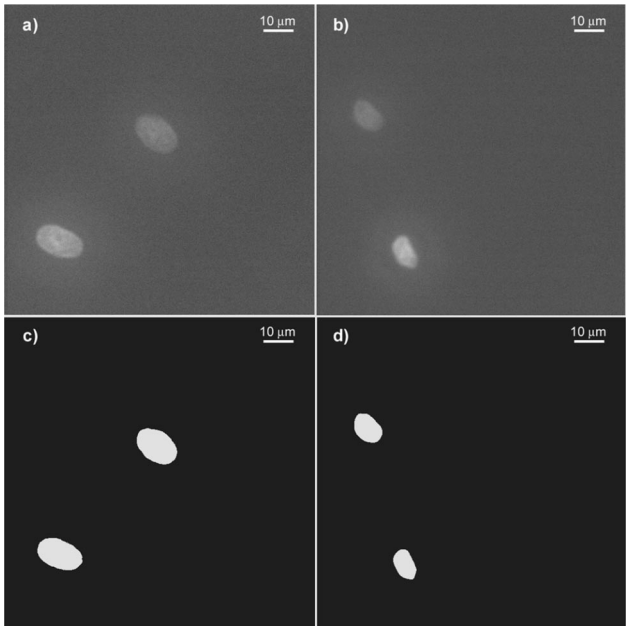

Fig. 3 Representative fluorescence images of the cell nuclei at time (*a*) $t=0$ s, and (*b*) $t=180$ s; and the corresponding processed images for (*c*) $t=0$ s, and (*d*) $t=180$ s

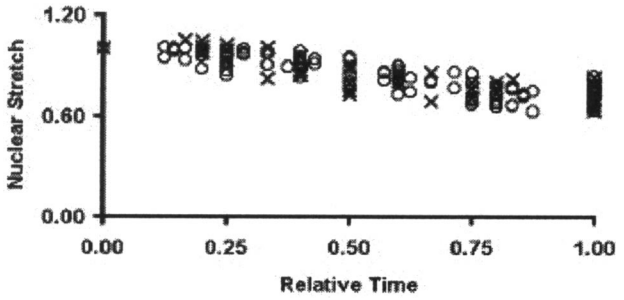

Fig. 4 Nuclear stretch as a function of relative time for 0.006% (X) and 0.017% (O) of trypsin

4 Estimation of the Forces Acting on the Nucleus

We used the measured nuclear stretches to estimate forces acting on the nucleus during cell rounding. Although the specific microstructure and properties of the cytoskeleton are not involved in our analysis, it is based on the scenario sketched in Fig. 8. In

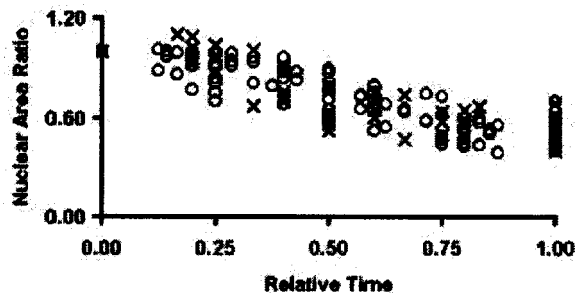

Fig. 5 Relative nuclear area change as a function of relative time for 0.006% (X) and 0.017% (O) of trypsin

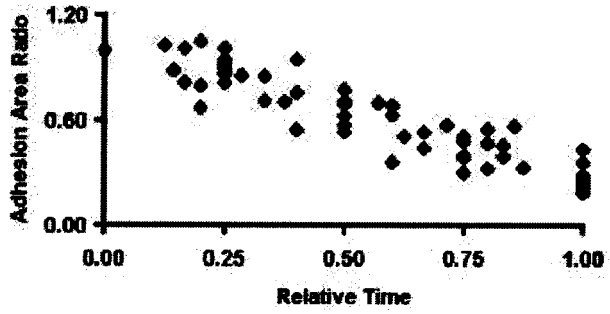

Fig. 6 Relative apparent adhesion area (projected area) change as a function of relative time for 0.017% trypsin (adhesion area ratio)

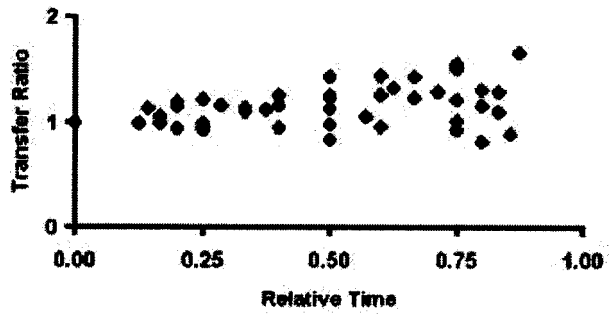

Fig. 7 Ratio of the nuclear area ratio to the adhesion area ratio as a function of relative time for 0.017% trypsin

Table 1 Values of the means and standard deviations of the nuclear area ratio in different relative time ranges for different final concentrations of trypsin, and combined data

	Trypsin concentration		
Relative time range	0.25 mg/ml	0.35 mg/ml	Combined data
0.10–0.35	0.97±0.13	0.92±0.09	0.93±0.10
0.36–0.63	0.71±0.11	0.75±0.12	0.74±0.12
0.64–0.90	0.60±0.08	0.54±0.09	0.56±0.09
1.00	0.55±0.08	0.50±0.07	0.52±0.08

order to understand the process of the nuclear deformation during cell rounding, we can first imagine the preprocess of cell spreading. The main part of the nuclear deformation is probably caused by an extension of the nucleus by cytoskeletal fibers attached to the adhesion sites, such as aggregations of focal adhesions [Figs. 8(*a*) and 8(*b*)], and the nature of the corresponding tensile forces is the interaction of the fiber with myosin motors. In the process of cell rounding, the extended (prestressed) state of the nucleus corresponding to the spread state of the cell is the reference state [Fig. 8(*c*)], and the more spherical (probably, free of stress) state of the nucleus corresponding to the round state is the final state [Fig. 8(*d*)]. Notice that, in our model, we consider the difference between the stresses in the final (round) and reference (spread) states, but not the initial stresses in the spread state. While, in principle, the initial stresses could influence the stress difference under consideration, the results of [31] in terms of hysteresis and variation of the nuclear Young's modulus during cell rounding show that this effect is, probably, small. This difference in stresses determines the nuclear stretches measured in our experiment. Physically, the rounding of the nucleus is caused by an inactivation of the fibers because the fibers lose their connections to adhesion sites when the cell detaches from the surface. From the standpoint of our model, it is equivalent to the application to the nucleus in the reference state of the forces opposite to those that extended the nucleus during cell spreading [Fig. 8(*d*)]. Such forces are directed along fibers that become inactive during cell rounding. The arguments similar to that presented here can be used in the analysis of initial and intermediate states. In such cases, the forces will be applied along a portion of the fibers inactivated due to a partial detachment of the cell.

Table 2 Values of the means and standard deviations of the adhesion area ratio in different relative time ranges for a trypsin concentration of 0.017%

	Trypsin concentration
Relative time range	0.35 mg/ml
0.10–0.35	0.88±0.11
0.36–0.63	0.66±0.13
0.64–0.90	0.45±0.09
1.00	0.28±0.07

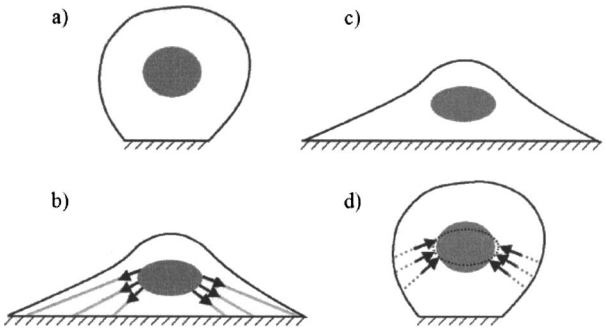

Fig. 8 Conceptual sketch of the estimation of the forces deforming the nucleus during cell rounding. (*A*) and (*b*) preprocess of cell spreading; (*a*) cell in the round state, and (*b*) cell in the spread state where the nucleus is deformed by the cytoskeletal fibers. (*C*) and (*d*) process of cell rounding; (*c*) the reference (spread and prestressed state) and (*d*) the final round state (solid line), in order to reach the round state the forces (arrows) are applied to the nucleus in the spread state (dashed line); the forces are directed along the fibers that become inactivated during cell rounding, and they are opposite to those that extended the nucleus to its spread state in the preprocess.

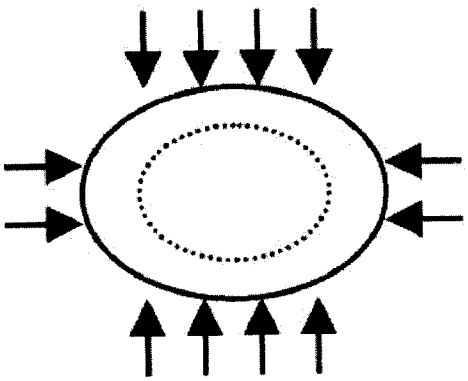

Fig. 9 The scheme to convert the stresses deforming the nucleus into a system of forces. In the model, the difference between the nuclear stresses in the final (round) and reference is analyzed, and the corresponding model forces appear as compressive. The application of these forces is equivalent to the effect of the loss of pretension. The contours of the projected areas of the nucleus in its spread and round states are given by the solid and dashed lines, respectively.

To derive the stresses and forces deforming the nucleus, we consider a layer of the nucleus parallel to the substrate where along the circumference the fibers are attached and the forces are applied. Figure 9 shows a cross section of the layer parallel to the adhesion site and the plane of imaging, including the projected areas of undeformed and deformed nuclei. We are interested here in the forces acting along the circumference of the layer (Fig. 9) as the forces primarily associated with the cytoskeleton (see our comment above). Certainly, the three-dimensional deformation of the layer under consideration is accompanied by forces acting along the top and bottom surfaces. These forces are a result of the response of the nuclear material to the application of the circumferential forces. The reactive forces along the top and bottom surfaces of the nuclear layer can be estimated on the basis of the strain energy function introduced below but we will not discuss them here.

To characterize the material of the nucleus (nuclear layer), we will use the model of a nonlinear compressible neo-Hookean material whose constitutive relations are based on the strain energy function [37]

$$W=\mu[(\lambda_1^*)^2+(\lambda_2^*)^2+(\lambda_3^*)^2-3]+K(J-1)^2 \tag{3}$$

where μ and K are shear modulus and bulk modulus, respectively, and λ_i^* $(i=1,2,3)$ are the principal deviatoric stretches related to the original principal stretches λ_i $(i=1,2,3)$ by the equation

$$\lambda_i^*=\lambda_i/J^{1/3} \tag{4}$$

Here, J is the relative volume change $(J=\lambda_1\lambda_2\lambda_3)$. On the basis of the introduced strain energy function, the principal stresses, t_i, inside the layer can be found as

$$t_i=J^{-1}\lambda_i\frac{\partial W}{\partial \lambda_i} \tag{5}$$

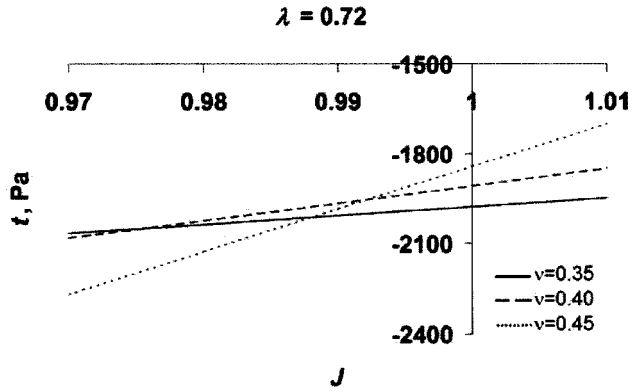

Fig. 10 Nuclear stress, *t*, as a function of the relative volume change, *J*, and Poisson's ratio, ν, corresponding to the round state

We interpret the major and minor axes of the elliptical cross section of the nucleus in the plane of imaging as principal axes. Based upon our observations during the trypsin experiments (see Discussion), we found the stretches in directions 1 and 2 (principal stretches) are equal, which means that the stretches in direction 1 and 2 are both equal to the square-root of the nuclear area ratio. We use the notation $\lambda_1=\lambda_2=\lambda$, and analyze the stresses in the layer as functions of the in-plane stretch λ and volume change *J*. We also express shear modulus and bulk modulus in terms of Young's modulus, *E*, and Poisson's ratio, ν. Taking this into account, the principal stresses can be expressed by the following equation:

$$t_1=t_2=t=J^{-1}\frac{E}{6(1+\nu)}(\lambda^2-J^2/\lambda^4)+\frac{E}{3(1-2\nu)}(J-1) \quad (6)$$

According to the scenario of cell rounding in Fig. 8, the stresses, *t*, characterize the cytoskeletal forces that act on the nucleus; they are maximal in the spread state of the cell and relax as a result of cell rounding. In Figs. 10 and 11, we present stresses, *t*, for two values of stretch: $\lambda=0.72$ (the round state); and, $\lambda=0.86$ (an intermediate state). We also varied the parameters of compressibility of the nucleus. The content of the nucleus has both solid-type (DNA/chromatin) and liquid-type phases. Because of that, we assume a certain compressibility of the nucleus. An experiment with compression of the fibroblast [38] has shown compressibility of the cellular nucleus. In Figs. 10 and 11, we analyzed the stress variation in the range between 3%-compression and 1%-expansion. On the basis of estimates [31], we chose the following value of Young's modulus

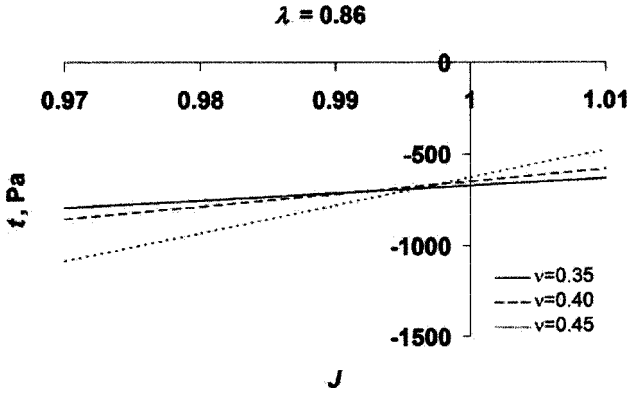

Fig. 11 Nuclear stress, *t*, as a function of the relative volume change, *J*, and Poisson's ratio, ν, corresponding to an intermediate state

Table 3 Values of the principle stretches, stresses, and equivalent forces in different relative time ranges. The stresses are converted into equivalent forces on the basis of a 2–4 μm height range for the band along which the cytoskeletal forces are assumed to be applied. The corresponding force ranges are presented in the table.

Relative time range	Principal stretches	Principal stresses, Pa	Forces, nN
0.10–0.35	0.96	−150	1.0–2.0
0.36–0.63	0.86	−700	4.9–9.8
0.64–0.90	0.75	−1600	10.0–20.0
1.00	0.72	−2000	14.0–28.0

$$E=5000 \text{ Pa} \quad (7)$$

In Figs. 10 and 11, we present the stress for 3 values (0.35, 0.40, and 0.45) of Poisson's ratio. The third principal stretch, λ_3, is determined by the in-plane stretches and compressibility of the nucleus, and it is given by the equation

$$\lambda_3=\frac{J}{\lambda_1\lambda_2} \quad (8)$$

It is common to characterize the cellular cytoskeletal machinery in terms of the produced force, e.g., [33]. In order to make a comparison with experimental data, where cellular forces were measured, we represent the stresses acting along the circumference of the nucleus by a system of a pair of two forces parallel to the long axes of the nucleus and four pairs of the forces parallel to the short axes of the nucleus. We convert the computed stresses into forces by considering different fractions of the nuclear surfaces to which the fibers are attached (see the discussion below). The values of the forces along with the corresponding stresses and stretches for different moments of time of the rounding are given in Table 3.

5 Discussion and Conclusion

Our study was motivated by the need for a better understanding of the role that mechanical characteristics play in signal transduction from the extracellular matrix to the cell. Here, we analyzed a cellular response elicited from mechanical force transmitted from the cell surface via the cytoskeleton to the nucleus.

Our main objective was to measure nuclear deformations during cell rounding, so we imaged the nucleus (Fig. 2) and cell adhesion area (Fig. 3) during the process. To facilitate analysis of these images, we converted their range of intensity values to binary. Our image processing was fairly automated for the nucleus (thresholding and level shifting), and accurately traced the structure. Manual outlining was used to trace the cell adhesion area. Due to the very large number of pixels contained in the cell adhesion areas (tens of thousands), accidental loss or addition of a few pixels due to errors in the manual outlining did not significantly affect our estimate of the relative change.

We selected to measure nuclear stretches, since this would exclude the effect of cell size, and provide a useful parameter when investigating the mechanics. We used two concentrations of trypsin to determine if the results were concentration-dependent. We also normalized the time of cell rounding for each cell to investigate any rate-dependence. In order to uniformly define the endpoint of rounding, we selected the following criteria: the middle frame of a triplet set of images of the nucleus where the difference in relative change in projected nuclear area was less than 4%, and the magnitude of the relative change in projected nuclear area was less than 75%.

When we measured nuclear stretch in directions 1 and 2 for $n=14$ cells for the round state, we found that the mean value of both stretches was the same (0.69). Since the stretches were the

same in each direction, this meant the square-root of the relative change in projected nuclear area was a fair measure of nuclear stretch in either direction.

Although we measured only in-plane deformation of the nucleus, a 3D rounding of the nucleus can be supported by the following argument. Assuming an elliptical shape and a slight compressibility of the nucleus, its height, λ_3, can be estimated as

$$\lambda_3 \approx \frac{1}{\lambda_1 \lambda_2} \tag{9}$$

In our experiment the in-plane axes shrink about 18%, and the normal axis becomes about twice as long. Thus an originally flattened nucleus becomes more spherical at the end of cell rounding. This is consistent with the morphometric data in [31], Fig. 3 on p. 180.

In our analysis, we measured the principal stretches of the projected nuclear area during endothelial cell rounding. Due to the nature of our imaging, we measure the nuclear cross-section that has the maximal area out of all horizontal planes. Thus, this area does not depend upon vertical position of the nucleus. Therefore, the principal stretches are also not sensitive to position of the nucleus in the vertical direction.

Figure 4 clearly shows that trypsin concentration and rate of rounding do not significantly affect the nuclear stretch. Similarly, the relative change in projected nuclear area is not sensitive to trypsin-concentration or rate of rounding, as seen in Fig. 5 (corresponding statistics in Table 1). Moreover, the closeness of the nuclear deformation parameters in Figs. 4 and 5 suggest that cell or nucleus size does not significantly affect the nuclear deformation. Next, we looked at the relative change in projected area (apparent adhesion area) as a function of relative time, shown in Fig. 6 (corresponding statistics in Table 2). All of these changes appear to have an approximately linear time course.

In order to compare the changes at the adhesion site and nucleus, we looked at the ratio of the relative change in projected nuclear area to the relative change in apparent adhesion area, given in Fig. 7. This transfer ratio had a value close to 1 for most of the process, with a slightly positive slope versus relative time. This suggests that the nuclear deformation is a direct and immediate response to changes in adhesion area. Additionally, since the transfer ratio possesses a slightly positive slope, this indicates that the nucleus is stiffer than the bulk cytosol/cytoskeleton, consistent with previous findings in [9,30].

In our model, we took into account the large deformation that the nucleus undergoes during the process of cell rounding. We also considered compressibility of the material of the nucleus caused by it structure. In application of our model to the estimation of the forces deforming the nucleus, we used the experimentally measured stretches and the stiffness modulus (Young's modulus) of the nucleus. We also assumed that the stresses and strains are homogeneous and the major axes of the cross sections of the nucleus coincide with the principal axes of the stress–strain state. Notice that these assumptions were applied only to the analysis of a nuclear layer that is presumably surrounded by cytoskeletal fibers. Also, we did not observe any significant rotations of the projected images of the nucleus that would indicate the presence of the shear mode of deformation.

We have recently developed a computational test of our analytical estimates of the stresses in the nucleus by using a 3D finite element simulation of the deformation of the nucleus under the action of stresses distributed along a band on its surface. While the full-scale computational results will be published elsewhere, we concluded that to reach compression of the nucleus consistent with our experimental results, applied stresses of about 2000 Pa are needed. This conclusion is consistent with our analytical results here (Figs. 10 and 11 and Table 3).

In our analysis here, the material of the nucleus is considered elastic. The viscoelastic properties of the endothelial cell nucleus are not available at the present time. In [30], such properties of the nuclei of chondrocytes were analyzed. The relaxation time has been found close to 25 s. The round state, which we compare here with the reference, extended, state is reached in about 180 s, a much longer time than the cited relaxation time. Furthermore, as we discussed earlier, we determined the round state as one when the projected area changed very little at three consecutive moments of time, which indicates that creep of the material is minimal. Thus, we can conclude that the effect of viscoelasticity on our results is, probably, insignificant.

Also, our modeling is based on an estimated value of the Young's modulus of the nucleus (5000 Pa). In principal, there could be a certain variation of this modulus during the cell transition from the spread to round state. This issue was addressed in [31], where the stiffness of endothelial cell nuclei was estimated for two, round and spread states of the cell. The estimated values were, respectively, about 4400 Pa and 5100 Pa. This means that the changes in the stiffness of the nucleus during the cell rounding are relatively small.

The obtained estimates have some variability depending on the characteristics of compressibility, J and ν. This variability is greater in the cases of small compressibility ($\nu \to 0.5$) and small λ. However, in the case of the comparison of the original spread state and the final round state, the changes in stress are quite limited, and $t = 2000$ Pa can be considered a reasonable estimate of the level of stress. When, the stresses are converted into forces, we make additional assumptions regarding the number of forces and the height of the band along which the forces are applied. A realistic estimate of the height of the endothelial cell's nucleus that corresponds to the spread state of the cell is about 5–8 μm (e.g., Fig. 3 on p. 180 in [31]). The fibers cannot anchor the nucleus along its whole surface: it would be inconsistent with their inclination with respect to the surface of the cell attachment. On the other hand, the fibers cannot take a very narrow band along the nuclear surface: to provide an about 2000 Pa level of stress it would result in an unreasonable force per fiber. Thus, we assume a range of the fiber/nucleus contact band about 2–4 μm that results in a range of the force about 14–28 nN. If we take into account the variability of all parameters involved in the force deforming the nucleus, it will still be a few tens of nanoNewtons.

Experimental information on the forces acting on the nucleus during cell rounding is unavailable at this time. Our biological interpretation of the process of the deformation of the nucleus is that cytoskeletal fibers attached to the nucleus and the adhesion site generate the forces deforming the nucleus (see also comments above). The machinery behind the generation of such forces is probably associated with actin/myosin interaction. Thus, the forces deforming the nucleus and forces acting along the adhesion site (traction forces), while not equal, have the same nature, and should be on the same order of magnitude. We looked at the estimates of the traction forces made by several groups. Numerous technologies have been used to study cell adhesion forces, including substrates consisting of thin silicon films [39–41], polyacrilamide sheets [42,43], novel micromachined devices [44], and elastic posts [12]. Various cell types, including BPASMCs, keratocytes, myocytes, and fibroblasts have been studied using these technologies, but as of yet, no endothelial cells. The estimated traction forces of these cells are: 20–100 nN for the BPASMCs [12]; 20–50 nN for keratocytes [13,14]; 70 nN for cardiac myocytes [15]; and, 20 nN–5000 nN for fibroblasts [15,16]. For the fibroblasts, the large traction force range can be attributed to the different cell subtypes and estimation techniques. Taken as a whole, these ranges of traction force are on the same order of magnitude as our estimate for the internal forces acting on the nucleus.

Recently, traction forces generated by endothelial cells have been studied in [45]. In particular, the relationship between traction forces and endothelial cell spreading has been investigated. It has been shown that overall force produced by the cell is a linear function of the adhesion area. Thus, if the cell retracts from a

more spread state to a more round state, traction forces relax. Traction forces and the internal forces acting on the nucleus are related via contractile forces generated by the cytoskeleton. Thus, the result of [45] is consistent with the scheme of the present paper where we consider the relaxation of the forces acting on the nucleus as a result of the cell rounding.

In this study, we found that alterations of the adhesion area of an endothelial cell results in deformation of the cell nucleus, and this is a direct and immediate relationship. Cell transition from the fully spread state to the round state is accompanied by significant nuclear deformation. The principal stretches of the nucleus corresponding to the projected nuclear area have the same mean value. We then estimated stresses and forces that produce the deformation of the nucleus at the level of 2000 Pa and 14–28 nN, respectively. This is on the same order of magnitude as experimentally measured traction forces. In general, these results can shed additional light on the mechanotransduction pathways in cells. In particular, they can help in understanding the active force generation in the cytoskeleton. The obtained results can also help in the characterization of the conditions of the nuclear envelope and nuclear content, and ultimately, in the understanding of the mechanism of gene alteration and protein synthesis involved in mechanotransduction. Finally, our analytical estimates are important for the development of comprehensive 3D computational models of cells interacting with their cellular environment.

Acknowledgments

We thank Dr. Micah Dembo for the discussions and valuable comments on the manuscript, and Dr. Wei-Chun Chin for his assistance with cell culture and imaging. The authors also thank the Whitaker Foundation, NIBIB (EB00262), and NHLBI (HL73305) for partial support of this investigation.

References

[1] Davies, P. F., Barbee, K. A., Volin, M. V., Robotewskyj, A., Chen, J., Joseph, L., Griem, M. L., Wernick, M. N., Jacobs, E., Polacek, D. C., dePaola, N., and Barakat, A. I., 1997, ''Spatial Relationships in Early Signaling Events of Flow-Mediated Endothelial Mechanotransduction,'' Annu. Rev. Physiol., **59**, pp. 527–549.

[2] Brighton, C. T., Fisher, J. R., Levine, S. E., Corsetti, J. R., Reilly, T., Landsman, A. S., Williams, J. L., and Thibault, L. E., 1996, ''The Biochemical Pathway Mediating the Proliferative Response of Bone Cells to a Mechanical Stimulus,'' Bone Joint Surg. A., Vol., **78**, pp. 1337–1347.

[3] Brownell, W. E., Spector, A. A., Raphael, R. M., and Popel, A. S., 2001, ''Micro- and Nanomechanics of the Cochlear Outer Hair Cell,'' Annu. Rev. Biomed. Eng., **3**, pp. 169–194.

[4] Gudi, S., Nolan, J. P., and Frangos, J. A., 1998, ''Modulation of GTPase Activity of G Proteins by Fluid Stress and Phospholipid Composition,'' Proc. Natl. Acad. Sci. U.S.A., **95**, pp. 2616–2619.

[5] Mathur, A. B., Truskey, G. A., and Reichert, W. M., 2000, ''Atomic Force and Total Internal Reflection Fluorescence Microscopy for the Study of Force Transmission in Endothelial Cells,'' Biophys. J., **78**, pp. 1725–1735.

[6] Mathur, A. B., Truskey, G. A., and Reichert, W. M., 2000, ''Total Internal Reflection Microscopy and Atomic Force Microscopy (TIRFM-AFM) to Study Stress Transduction Mechanisms in Endothelial Cells,'' Crit. Rev. Biomed. Eng., **28**, pp. 197–202.

[7] Juliano, R. L., and Haskill, S., 1993, ''Signal Transduction From the Extracellular Matrix,'' J. Cell Biol., **120**, pp. 577–585.

[8] Davies, P. F., 1995, ''Flow-Mediated Endothelial Mechanotransduction,'' Physiol. Res., **75**, pp. 519–560.

[9] Maniotis, A. J., Chen, C. S., and Ingber, D. E., 1997, ''Demonstration of Mechanical Connections Between Integrins, Cytoskeletal Filaments, and Nucleoplasm That Stabilize Nuclear Structure,'' Proc. Natl. Acad. Sci. U.S.A., **94**, pp. 849–854.

[10] Thomas, C. H., Collier, J. H., Sfeir, C. S., and Healy, K. E., 2002, ''Engineering Gene Expression and Protein Synthesis by Modulation of Nuclear Shape,'' Proc. Natl. Acad. Sci. U.S.A., **99**, pp. 1972–1977.

[11] Chicurel, M. E., Chen, C. S., and Ingber, D. E., 1998, ''Cellular Control Lies in the Balance of Forces,'' Curr. Opin. Cell Biol., **10**, pp. 232–239.

[12] Tan, J. L., Tien, J., Pirone, D. M., Gray, D. S., Bhadriraju, K., and Chen, C. S., 2003, ''Cells Lying on a bed of Microneedles: An Approach to Isolate Mechanical Force,'' Proc. Natl. Acad. Sci. U.S.A., **100**, pp. 1484–1489.

[13] Lee, J., Leonard, M., Oliver, T., Ishihara, A., and Jacobson, K., 1994, ''Traction Forces Generated by Locomoting Keratocytes,'' J. Cell Biol., **127**, pp. 1957–1964.

[14] Oliver, T., Dembo, M., and Jacobson, K., 1995, ''Traction Forces in Locomoting Cells,'' Cell Motil. Cytoskeleton, **31**, pp. 225–240.

[15] Balaban, N. Q., Schwarz, U. S., Riveline, D., Goichberg, P., Tzur, G., Sabanay, I., Mahalu, D., Safran, S., Bershadsky, A., Addadi, L., and Geiger, B., 2001, ''Force and Focal Adhesion Assembly: A Close Relationship Studied Using Elastic Micropatterned Substrates,'' Nat. Cell Biol., **3**, pp. 466–472.

[16] Wang, H. B., Dembo, M., Hanks, S. K., and Wang, Y.-L., 2001, ''Focal Adhesion Kinase in Involved in Mechanosensing During Fibroblast Migration,'' Proc. Natl. Acad. Sci. U.S.A., **98**, pp. 11295–11300.

[17] Ingber, D., 1997, ''Tensegrity: The Architectural Basis of Cellular Mechanotransduction,'' Annu. Rev. Physiol., **59**, pp. 575–599.

[18] Girard, P. R., and Nerem, R. M., 1995, ''Shear Stress Modulates Endothelial Cell Morphology and F-Actin Organization Through the Regulation of Focal Adhesion-Associated Proteins,'' J. Cell Physiol., **163**, pp. 179–193.

[19] Finer, J. T., Simmons, R. M., and Spudich, J. A., 1994, ''Single Myosin Molecule Mechanics: Piconewton Forces and Nanometre Steps,'' Nature (London), **368**, pp. 113–119.

[20] Helmke, B. P., Goldman, R. D., and Davies, P. F., 2000, ''Rapid Displacement of Vimentin Intermediate Filaments in Living Endothelial Cells Exposed to Flow,'' Circ. Res., **86**, pp. 745–752.

[21] Helmke, B. P., Rosen, A. B., and Davies, P. F., 2003, ''Mapping Mechanical Strain of an Endogenous Cytoskeletal Network in Living Endothelial Cells,'' Biophys. J., **84**, pp. 2691–2699.

[22] Dembo, M., Maltrud, M., and Harlow, F., 1986, ''Numerical Studies of Unreactive Contractile Networks,'' Biophys. J., **50**, pp. 123–137.

[23] Satcher, R. L., and Dewey, C. F., 1996, ''Theoretical Estimates of Mechanical Properties of the Endothelial Cell Cytoskeleton,'' Biophys. J., **71**, pp. 109–118.

[24] Boey, S. K., Beal, D. H., and Discher, D. E., 1998, ''Simulations of the Erythrocyte Cytoskeleton at Large Deformation. I. Microscopic Models,'' Biophys. J., **75**, pp. 1573–1583.

[25] Hansen, J. C., Skalak, R., Chien, S., and Hoger, A., 1997, ''Influence of Network Topology on the Elasticity of the Red Blood Cell Membrane Skeleton,'' Biophys. J., **72**, pp. 2369–2381.

[26] Hansen, J. C., Skalak, R., Chien, S., and Hoger, A., 1997, ''Spectrin Properties and the Elasticity of the Red Blood Cell Membrane Skeleton,'' Biorheology, **34**, pp. 327–348.

[27] Civelekoglu, G., and Edelstein-Keshet, L., 1994, ''Modelling the Dynamics of F-Actin in the Cell,'' Bull. Math. Biol., **56**, pp. 587–616.

[28] Geigant, E., Ladizhansky, K., and Mogilner, A., 1998, ''An Integro-Differential Model for Orientational Distribution of F-Actin in Cells,'' SIAM (Soc. Ind. Appl. Math.) J. Appl. Math., **59**, pp. 787–809.

[29] Spector, A. A., Ameen, M., Charalambides, P. G., and Popel, A. S., 2002, ''Nanostructure, Effective Properties, and Deformation Pattern of the Cochlear Outer Hair Cell Cytoskeleton,'' J. Biomech. Eng., **124**, pp. 180–187.

[30] Guilak, F., Tedrow, J. R., and Burgkart, R., 2000, ''Viscoelastic Properties of the Cell Nucleus,'' Biochem. Biophys. Res. Commun., **269**, pp. 781–786.

[31] Caille, N., Thoumine, O., Tardy, Y., and Meister, J. J., 2002, ''Contribution of the Nucleus to the Mechanical Properties of Endothelial Cells,'' J. Biomech., **35**, pp. 177–187.

[32] Theret, D. P., Levesque, M. J., Sato, M., Nerem, R. M., and Wheeler, L. T., 1988, ''The Application of a Homogenous Half-Space Model in the Analysis of Endothelial Cell Micropipette Measurements,'' J. Biomech. Eng., **110**, pp. 190–199.

[33] Shafrir, Y., and Forgacs, G., 2002, ''Mechanotransduction Through the Cytoskeleton,'' Am. J. Physiol. Cell Physiol., **282**, pp. C479–C486.

[34] Hazel, A. L., and Pedley, T. J., 2000, ''Vascular Endothelial Cells Minimize the Total Force on Their Nuclei,'' Biophys. J., **78**, pp. 47–54.

[35] Pienta, K. J., and Coffey, D. S., 1992, ''Nuclear-Cytoskeletal Interactions: Evidence for Physical Connections Between the Nucleus and Cell Periphery and Their Alteration by Transformation,'' J. Cell. Biochem., **49**, pp. 357–365.

[36] Sims, J. R., Karp, S., and Ingber, D. E., 1992, ''Altering the Cellular Mechanical Force Balance Results in Integrated Changes in Cell, Cytoskeletal and Nuclear Shape,'' J. Cell. Sci., **103**, pp. 1215–1222.

[37] Ogden, R. W., 1997, *Nonlinear Elastic Deformations*, 2nd ed., Dover, Mineola.

[38] Guilak, F., 1995, ''Compression-Induced Changes in the Shape and Volume of the Chondrocyte Nucleus,'' J. Biomech., **28**, pp. 1529–1541.

[39] Harris, A. K., Wild, P., and Stopak, D., 1980, ''Silicone Rubber Substrata: a New Wrinkle in the Study of Cell Locomotion,'' Science, **208**, pp. 177–179.

[40] Harris, A. K., Stopak, D., and Wild, P., 1981, ''Fibroblast Traction as a Mechanism for Collage Morphogenesis,'' Nature (London), **290**, pp. 249–251.

[41] Burton, K., and Taylor, D. L., 1997, ''Traction Forces of Cytokinesis Measured With Optically Modified Substrata,'' Nature (London), **385**, pp. 450–454.

[42] Pelham, R. J., and Wang, Y.-L., 1997, ''Cell Locomotion and Focal Adhesions are Regulated by Substrate Flexibility,'' Proc. Natl. Acad. Sci. U.S.A., **94**, pp. 13661–13665.

[43] Beningo, K. A., and Wang, Y.-L., 2002, ''Flexible Polyacrylamide Substrates for the Analysis of Mechanical Interactions at Cell-Substrate Adhesions,'' Methods Cell Biol., **69**, pp. 325–339.

[44] Galbraith, C. G., and Sheetz, M. P., 1997, ''A Micromachined Device Provides a New Bend on Fibroblast Traction Forces,'' Proc. Natl. Acad. Sci. U.S.A., **94**, pp. 9114–9118.

[45] Reinhart-King, C. A., Dembo, M., and Hammer, D. A., 2003, ''Endothelial Cell Traction Forces on RGD-Derivatized Polyacrylamide Substrata,'' Langmuir, **19**, pp. 1573–1579.